poorer agreement with experiment. However, not too much should be made of this given the uncertain conditions of commercial diketene formation. About all that should be said is that, in a rough way, calculations of the kinetic isotope effects are in accord with Pascal's observed deuterium ratios. The experimental measurement of these isotope effects at a known temperature would be worthwhile.

A minor point concerns Pascal's comment that $(a + a')/b = 0.975$ suggests an inverse secondary kinetic isotope effect for the dimerization of ketene. Although Table III shows that kinetic isotope effects on the rate of diketene formation are computed to be inverse for all positions of deuterium substitution, this conclusion does not seem to follow from Pascal's results. Table III also lists several kinetic isotope effects of oxygen and carbon isotopomers.

Finally, a point of Pascal's that is strongly supported by our calculations is his tentative assignment of H_a in diketene as the hydrogen cis to the ring oxygen and $H_{a'}$ as cis to the ring carbon. With this assumption, all our calculations give $a'/a > 1$, as found by experiment.

Acknowledgment. We thank the Fulbright Program for a Fellowship to I.G. during the tenure of which this work was carried out. We are also grateful to the National Science Foundation for a grant (CHE 8808018) that allowed the purchase of our SCS 40 computer.

Effect of Electron Correlation on the Electrostatic Potential Distribution of Molecules

F. J. Luque,*,† M. Orozco,‡ F. Illas,§ and J. Rubio§

Contribution from the Departament de Farmacia, Unitat Fisicoquimica, Facultat de Farmàcia, Universitat de Barcelona, Avgda. Diagonal s/n, 08028 Barcelona, Spain, and Departament de Bioquimica i Fisiologia and Departament de Quimica Fisica, Facultat de Quimica, Universitat de Barcelona, C/. Martí i Franques 1, 08028 Barcelona, Spain. *Received September 19, 1990*

Abstract: A study on the effect of the electron correlation on the electrostatic potential distribution in molecules is presented. The study is focused not only on the features of the molecular electrostatic potential (MEP), but also on the atomic charges and dipoles. Electron correlation is introduced by means of the CIPSI and full-CI methods by using both 6-31G* and 6-31G basis sets. The results reported in this paper clearly point out the reliability of the CIPSI method to reproduce the features of the MEP evaluated from full-CI wave functions. Comparison of MEPs computed from SCF and full-CI wave functions indicates that the electron correlation does not have a uniform effect on the MEP in the whole space surrounding the molecule. Thus, electron correlation has a relevant effect near the nuclei, but the MEP determined from the SCF wave function remains largely unaffected in regions located outside the van der Waals sphere. Indeed, the characteristics of the SCF MEP minima undergo only a small change when electron correlation is considered.

Introduction

The inclusion of electron correlation in quantum chemical studies is becoming a usual practice due to the need for precisely determining both the total energy and the molecular properties. One of these properties is electron density, which is highly informative about the reactivity characteristics of molecules. Since the early quantum chemical studies, a large amount of research effort has been focused on the description of the electron density distribution and other related molecular properties within the Hartree-Fock framework. Nevertheless, less attention has been devoted to determine the influence of the electron correlation on the electron density,[1] even though this effect is expected to be essential in order to obtain a reliable picture of the electron density distribution and of related molecular properties.[2]

After the early work of Daudel et al.,[2b] several studies on the electron correlation modulation of properties related to the molecular electrostatic distribution have been reported. Amos et al.[3] investigated the changes in the molecular multipole moments computed from configuration interaction and perturbation theory with regard to those evaluated at the SCF level. Hehre et al.[4] and Cioslowski[5] recently examined the effect of the electron correlation on atomic charges by means of calculations at both SCF and second-order Moller-Plesset levels. However, to our knowledge, systematic studies on the effect of the electron correlation on the electrostatic distribution have not previously been reported.

The relevance of the molecular electrostatic potential (MEP) in determining chemical reactivity has been stressed elsewhere.[6-11]

† Departament de Farmàcia.
‡ Departament de Bioquimica i Fisiologia.
§ Departament de Quimica Fisica.

(1) (a) Wang, L. C.; Boyd, R. J. *J. Chem. Phys.* **1989**, *90*, 1083. (b) Boyd, R. J.; Wang, L. C. *J. Comput. Chem.* **1989**, *10*, 367. (c) Gatti, C.; MacDougall, D. J.; Bader, R. F. W. *J. Chem. Phys.* **1988**, *88*, 3792 and references therein.
(2) Szabó, A.; Ostlund, N. S. *Modern Quantum Chemistry*; MacMillan: New York, 1982. (b) Daudel, R.; LeRouzo, H.; Cimiraglia, R.; Tomasi, J. *Int. J. Quantum Chem.* **1978**, *13*, 537.
(3) (a) Amos, R. D. *Chem. Phys. Lett.* **1980**, *73*, 602. (b) Amos, R. D. *Chem. Phys. Lett.* **1985**, *113*, 19.
(4) Carpenter, J. E.; McGrath, M. P.; Hehre, W. J. *J. Am. Chem. Soc.* **1989**, *111*, 6154.
(5) Cioslowski, J. *J. Am. Chem. Soc.* **1989**, *111*, 8333.
(6) Scrocco, E.; Tomasi, J. *Top. Curr. Chem.* **1973**, *42*, 95.
(7) (a) Politzer, P.; Daiker, K. C. In *The Force Constant in Chemistry*; Deb, B. M., Ed.; Van Nostrand Reinhold: New York, 1981; p 294. (b) *Chemical Applications of Atomic and Molecular Electrostatic Potentials*; Politzer, P., Truhlar, D. G., Eds.; Plenum Press: New York, 1981. (c) Náray-Szabó, G.; Surján, P. R. In *Theoretical Chemistry of Biological Systems*; Náray-Szabó, G., Ed.; Elsevier: Amsterdam, 1986; p 1.
(8) (a) Kollman, P.; McKelvey, J.; Johansson, A.; Rothenberg, S. *J. Am. Chem. Soc.* **1975**, *97*, 955. (b) Kollman, P.; Rothenberg, S. *J. Am. Chem. Soc.* **1977**, *99*, 1333. (c) Kollman, P. *J. Am. Chem. Soc.* **1977**, *99*, 4875. (d) Scrocco, E.; Tomasi, J. *Adv. Quantum Chem.* **1978**, *11*, 115. (e) Náray-Szabó, G. *Acta Phys. Acad. Sci. Hung.* **1981**, *51*, 65. (f) Politzer, P.; Landry, S. J.; Warnheim, T. *J. Phys. Chem.* **1982**, *86*, 4767. (g) Politzer, P.; Abrahmsen, L.; Sjoberg, P. *J. Am. Chem. Soc.* **1984**, *106*, 855.

0002-7863/91/1513-5203$02.50/0

Thus, the MEP has been widely used as a reactivity index in a large number of chemical research fields, such as molecular reactivity[6,7] particularly in the study of noncovalent interactions,[8] biological interactions,[9] solvation phenomena,[10] and electron density studies.[11]

The MEP is the rigorous quantum mechanical expectation value of the operator r^{-1}, it being defined at a point r by eq 1.[6]

$$V(r) = \sum_A \frac{Z_A}{|r - r_A|} - \int \frac{\rho(r_1)}{|r - r_1|}\, dr_1 \qquad (1)$$

The first term in the right hand of eq 1 reflects the nuclear electrostatic contribution of the point nuclear charges, Z_A, located at positions r_A, whereas the second term corresponds to the electrostatic potential originated from the molecular electron density, $\rho(r_1)$, extended in the whole space. Within the MO-LCAO framework, eq 1 adopts the form

$$V(r) = \sum_A \frac{Z_A}{|r - r_A|} - \sum_\mu \sum_\nu P_{\mu\nu} \int \frac{\chi_\mu(r_1)\chi_\nu(r_1)}{|r - r_1|}\, dr_1 \qquad (2)$$

where $P_{\mu\nu}$ is the element $\mu\nu$ of the first-order density matrix and χ denotes the atomic orbital basis set.

All the studies on the MEP reported in the literature have been carried out within the ab initio and semiempirical SCF framework, the main interest lying on the dependence of the MEP on the approximation level used in the computation of the SCF wave function. At this point, a large number of studies focused on the dependence of the ab initio MEP on the quality of the basis set used have been reported.[9c,12] Moreover, various strategies are available to compute the MEP from semiempirical wave functions.[7b,c,9c,12e,g,13]

Since the MEP is defined as the expectation value of a one-electron operator, it was assumed, even though not demonstrated, that the MEP will only exhibit very small differences when adding more Slater determinants to the SCF monodeterminantal wave function. Nevertheless, it is interesting to determine the confidence level of this assumption. Accordingly, we examine the effect of the electron correlation on the electrostatic potential evaluated in the space surrounding the molecule, particular attention being focused on the well depth and the location of the MEP minima.

Another aspect explored in the present study concerns the dependence of the partial atomic charges on the electron correlation. Partial atomic charges represent an attempt to condense the molecular charge distribution into a set of point charges usually located at the nuclei. Atomic charges provide a simple, intuitive way to rationalize chemical reactivity. However, their reliability has been seriously criticized, since atomic charge is not an exactly defined physical property, and consequently it must be evaluated by means of the approximate partitioning of the electronic charge distribution.

Several strategies have been formulated to compute atomic charges, either from empirical values or Huckel calculations[14] or from more sophisticated quantum mechanical molecular wave functions.[15] One widely used method for partitioning the electronic charge distribution is the Mulliken population analysis.[15a] The popularity of this method stems mainly from its computational simplicity, but its shortcomings are well-known.[15b,d,16,17] In the last decade, a strategy to calculate atomic charges (electrostatic charges) was proposed.[15b] According to this strategy, the charges are obtained by fitting the Coulombic monopole–monopole electrostatic potential, V^c, to the quantum mechanical electrostatic potential (eq 3 and 4). The high ability of electrostatic charges,

$$V^c(r) = \sum_i \frac{q_i}{|r - R_i|} \qquad (3)$$

$$\sum_j [V(r_j) - V^c(r_j)]^2 = \text{minimum} \qquad (4)$$

computed either from ab initio[16] or from semiempirical[17] wave functions, to represent the electrostatic interaction energy explains their inclusion in several force fields used in molecular mechanics and dynamics studies, like those of Kollman's group.[18]

Finally, our last objective was to determine the influence of the electron correlation on the dipole moment, a parameter that provides information about the molecular charge distribution. The dipole moment can be rigorously computed as the expectation value of the operator r, but it can also be approximately evaluated from the atomic charge distribution. Moreover, since the experimental gas-phase dipole moment can be accurately measured, the reliability of the dipole moment computed either from the wave function, whatever the method used in its computation (one-determinant SCF, many-determinant CI, etc.), or from atomic charges can be determined by comparison with the gas-phase experimental values.

Methods

In this paper, the effect of the electron correlation on the MEP has been studied by means of computations performed at the SCF level and by considering many-determinantal wave functions obtained by means of the CIPSI[19] and full-CI[20] methods. CIPSI calculations were carried out with the HONDO-CIPSI package.[21] Full-CI computations were per-

(9) (a) Hayes, D. M.; Kollman, P. A. *J. Am. Chem. Soc.* **1976**, *98*, 3335. (b) Hayes, D. M.; Kollman, P. A. *J. Am. Chem. Soc.* **1976**, *98*, 7811. (c) Petrongolo, C. *Gazz. Chim. Ital.* **1978**, *108*, 445. (d) Weiner, P. K.; Langridge, R.; Blaney, J. M.; Schaefer, R.; Kollman, P. A. *Proc. Natl. Acad. Sci. U.S.A.* **1982**, *79*, 3754. (e) Komatsu, K.; Nakamura, H.; Nakagawa, S.; Umeyama, H. *Chem. Pharm. Bull.* **1984**, *32*, 3313. (f) Náray-Szabó, G. *J. Mol. Struct.: THEOCHEM* **1986**, *138*, 197. (g) Luque, F. J.; Illas, F.; Pouplana, R. *Mol. Pharmacol.* **1987**, *32*, 557. (h) Náray-Szabó, G.; Nagy, P. *Int. J. Quantum Chem.* **1989**, *35*, 215. (i) Orozco, M.; Canela, E. I.; Franco, R. *J. Org. Chem.* **1990**, *55*, 2630. (j) Orozco, M.; Canela, E. I.; Franco, R. *Eur. J. Biochem.* **1990**, *188*, 155.

(10) (a) Oliveira Neto, M. *J. Comput. Chem.* **1986**, *7*, 617. (b) Oliveira Neto, M. *J. Comput. Chem.* **1986**, *7*, 629. (c) Bonaccorsi, R.; Cimiraglia, K.; Tomasi, J. *J. Comput. Chem.* **1983**, *4*, 567. (d) Davis, M. E.; McCammon, J. A. *Chem. Rev.* **1990**, *90*, 509. (e) Langlet, J.; Claverie, P.; Caillet, J.; Pullman, A. *J. Phys. Chem.* **1988**, *92*, 1617.

(11) (a) Politzer, P. *J. Chem. Phys.* **1980**, *72*, 3027. (b) Gadre, S. R.; Bendale, R. D. *Chem. Phys. Lett.* **1986**, *130*, 515. (c) Arteca, G. A.; Jammal, U. B.; Mezey, P. G. *J. Comput. Chem.* **1988**, *9*, 608.

(12) (a) Edwards, W. D.; Weinstein, H. *Chem. Phys. Lett.* **1978**, *56*, 582. (b) Mó, O.; Yáñez, M. *Theor. Chim. Acta* **1978**, *47*, 263. (c) Ramos, M. J.; Webster, B. *J. Chem. Soc., Faraday Trans. 2* **1983**, *79*, 1389. (d) Webster, B.; Hilczer, M.; Ramos, M. J.; Carmichael, J. *J. Chem. Soc., Faraday Trans. 2* **1985**, *81*, 1761. (e) Culberson, J. C.; Zerner, M. C. *Chem. Phys. Lett.* **1985**, *122*, 436. (f) Orozco, M.; Luque, F. J. *Chem. Phys. Lett.* **1989**, *160*, 305. (g) Luque, F. J.; Illas, F.; Orozco, M. *J. Comput. Chem.* **1990**, *11*, 416.

(13) (a) Giessner-Prettre, C.; Pullman, A. *Theor. Chim. Acta* **1972**, *25*, 83. (b) Srebrenick, S.; Weinstein, H.; Pauncz, R. *Chem. Phys. Lett.* **1973**, *20*, 419. (c) Giessner-Prettre, C.; Pullman, A. *Theor. Chim. Acta* **1974**, *33*, 91. (d) Giessner-Prettre, C.; Pullman, A. *Theor. Chim. Acta* **1975**, *37*, 335. (e) Duben, A. J. *Theor. Chim. Acta* **1981**, *59*, 81. (f) Luque, F. J.; Orozco, M. *Chem. Phys. Lett.* **1990**, *168*, 269.

(14) (a) Smith, R. P.; Ree, T.; Magee, J. L.; Eyring, H. *J. Am. Chem. Soc.* **1951**, *73*, 2263. (b) Del Re, G. *J. Chem. Soc.* **1958**, 4031. (c) Allinger, N. L.; Wuesthoff, T. *Tetrahedron* **1977**, *33*, 3. (d) Abraham, R. J.; Griffiths, L.; Loftus, P. *J. Comput. Chem.* **1982**, *3*, 407. (e) Lavery, R.; Zakrzewska, K.; Pullman, A. *J. Comput. Chem.* **1984**, *5*, 363. (f) Mullay, J. *J. Comput. Chem.* **1988**, *9*, 399.

(15) (a) Mulliken, R. S. *J. Chem. Phys.* **1962**, *36*, 3428. (b) Momany, F. A. *J. Phys. Chem.* **1978**, *82*, 592. (c) Wiberg, K. B. *J. Am. Chem. Soc.* **1979**, *101*, 1718. (d) Reed, A. E.; Weinstoch, R. B.; Weinhold, F. *J. Chem. Phys.* **1985**, *83*, 735. (e) Karafiloglou, P. *Chem. Phys.* **1988**, *128*, 373.

(16) (a) Cox, S. R.; Williams, D. E. *J. Comput. Chem.* **1981**, *2*, 304. (b) Singh, U. C.; Kollman, P. A. *J. Comput. Chem.* **1984**, *5*, 129. (c) Chirlian, L. E.; Francl, M. E. *J. Comput. Chem.* **1987**, *8*, 894. (d) Williams, D. E. *J. Comput. Chem.* **1988**, *9*, 745. (e) Woods, R. J.; Khalil, M.; Pell, W.; Moffat, S. H.; Smith, V. H., Jr. *J. Comput. Chem.* **1990**, *11*, 297. (f) Williams, D. E.; Yan, J. *Adv. At. Mol. Phys.* **1987**, *23*, 87.

(17) (a) Ferenczy, G. G.; Reynolds, C. A.; Richards, W. G. *J. Comput. Chem.* **1990**, *11*, 159. (b) Besler, B. H.; Merz, K. M.; Kollman, P. A. *J. Comput. Chem.* **1990**, *11*, 431. (c) Orozco, M.; Luque, F. J. *J. Comput. Chem.* **1990**, *11*, 909. (d) Orozco, M.; Luque, F. J. *J. Comput.-Aided Mol. Des.* **1990**, *4*, 411.

(18) (a) Weiner, P. K.; Kollman, P. A. *J. Comput. Chem.* **1981**, *2*, 287. (b) Weiner, S.; Kollman, P. A.; Case, D. A.; Singh, U. C.; Ghio, C.; Alagona, G.; Profeta, S., Jr.; Weiner, P. *J. Am. Chem. Soc.* **1984**, *106*, 765. (c) Weiner, S. J.; Kollman, P. A.; Nguyen, D. T.; Case, D. A. *J. Comput. Chem.* **1986**, *7*, 230.

(19) (a) Huron, B.; Malrieu, J. P.; Rancurel, P. *J. Chem. Phys.* **1973**, *58*, 5745. (b) Evangelisti, S.; Daudey, J. P.; Malrieu, J. P. *Chem. Phys.* **1983**, *75*, 91.

(20) Knowles, P. J.; Handy, N. C. *Chem. Phys. Lett.* **1984**, 111, 315.

(21) Dupuis, M.; Rys, J.; King, H. F. HONDO-76, program 338, QCPE; University of Indiana: Bloomington, IN 47401; pseudopotential adaptation by J. P. Daudey and M. Pelissier; general ROHF adaptation by R. Caballol and J. P. Daudey; CIPSI chain of programs by M. Pelissier, J. P. Daudey, S. Evangelisti, F. Spiegelmann, D. Maynou, F., Illas, and J. Rubio.

formed with a locally modified version[22] of the Knowles and Handy[23] full-CI code.

The characteristics of the CIPSI method have been discussed in detail elsewhere,[24] and consequently only the main features of the CIPSI algorithm will be described here. The procedure on which the CIPSI method is based consists of the definition of a space of generator determinants $\{G\}$. The Hamiltonian matrix representation of the $\{G\}$ space is diagonalized, and its eigenvectors define an initial zero-order wave function $|\psi_m^{(0)}\rangle$. Each determinant belonging to $\{G\}$ brings forth all single and double excitations. The contribution of each generated determinant to the first-order wave function is obtained according to the Epstein–Nesbet[25] partition of the electronic hamiltonian. Those generated determinants $\{GD\}$ contributing to the first-order wave function by a coefficient higher than a certain threshold value (ζ) are added to $\{G\}$, which is iteratively improved until no determinants are generated with a coefficient greater than ζ.

Since the number of generated determinants is usually very large, it is inconvenient to consider their entire contribution to the total energy by simple second-order perturbation theory. To solve this difficulty, a third class of determinants selected by means of a second test, denoted by the threshold parameter τ, has been defined.[19b] Thus, only those determinats of the $\{GD\}$ space contributing to the first-order wave function by a coefficient higher than τ are selected and included in the space $\{M\}$.

Then, the correlation energy recovered by the CIPSI method arises from two different contributions: (i) A variational term is obtained by diagonalizing the Hamiltonian matrix representation in the $\{G\} + \{M\}$ space and (ii) a perturbational contribution is taken into account up to the second order by means of the barycentric Moller–Plesset partition of the electronic Hamiltonian[19] including only the $\{GD\} - \{M\}$ determinants.

The zero-order one-particle density matrix is obtained as

$$\Gamma_{ij}^{(0)} = \langle \psi_m^{(0)} | \hat{i}^+ \hat{j} | \psi_m^{(0)} \rangle \qquad (5)$$

where i^+ and j stand for the corresponding creation and annihilation operators for spin orbitals $|\varphi_i\rangle$ and $|\varphi_j\rangle$, respectively. From these matrices, the natural orbitals[26] can then be obtained and used to compute the MEP according to eq 1.

In this paper, the electron correlation has been introduced by means of the CIPSI method at three different levels, which correspond to the evaluation of natural orbitals from the wave function determined from the diagonalization of the matrix representation of (i) the $\{G\}$ space, (ii) the $\{G\}$ space plus all the single excitations on $\{G\}$, and (iii) the $\{G\} + \{M\}$ space. These levels will be denoted in the text as CIPSI/G, CIPSI/G+S and CIPSI/G+M, respectively. In the present work, a value of ζ approximately 0.013 was chosen, thus leading to a $\{G\}$ space of 376 determinants for the largest case, whereas the value of τ selected as the dimension of the $\{G\} + \{M\}$ space was about 10 000 determinants.

SCF, CIPSI, and full-CI computations were performed for HF and H_2O by using the 6-31G[27] basis set with and without the frozen-core approximation, i.e., the freezing of the 1s electrons of non-hydrogen atoms. The same computations were carried out for HF by using the 6-31G*[28] basis set and the frozen-core approximation. In addition, SCF and CIPSI calculations were performed for H_2O, CO, N_2, HCN, and CH_2O with use of the 6-31G* basis set with the frozen-core approximation. The experimental geometries[29] of all the molecules were considered.

Table I. Difference in Total Energy,[a] ΔE (hartrees), and Well Depth, MEP Minimum (kcal/mol), of the Molecular Electrostatic Potential and Its Location (au) of HF[b]

	ΔE[c]	x	y	z	MEP minumum
		6-31G*			
SCF	0.000000	−1.15	0.00	−1.97	−34.48
CIPSI/G	−0.089950	−1.14	0.00	−1.99	−33.88
CIPSI/G+S	−0.091485	−1.07	0.00	−2.03	−32.50
CIPSI/G+M	−0.183613	−1.10	0.00	−2.02	−32.87
full-CI	−0.185553	−1.10	0.00	−2.02	−32.87
		6-31G			
SCF	0.000000	−1.55	0.00	−1.57	−45.10
CIPSI/G	−0.049164	−1.54	0.00	−1.59	−44.17
CIPSI/G+S	−0.049957	−1.46	0.00	−1.69	−41.35
CIPSI/G+M	−0.131304	−1.47	0.00	−1.67	−42.11
full-CI	−0.132310	−1.47	0.00	−1.68	−42.19
		6-31G[d]			
SCF	0.000000	−1.55	0.00	−1.57	−45.10
CIPSI/G	−0.049164	−1.54	0.00	−1.59	−44.17
CIPSI/G+S	−0.049952	−1.46	0.00	−1.69	−41.34
CIPSI/G+M	−0.130429	−1.47	0.00	−1.67	−42.11
full-CI	−0.131402	−1.46	0.00	−1.68	−42.09

[a] Referred to the energy computed at the SCF level. [b] Computations at the 6-31G* level were performed with the frozen-core approximation. The molecular geometry is given in ref 32. [c] E_{SCF}(6-31G*) = −100.000 747 hartrees; E_{SCF}(6-31G) = −99.983 409 hartrees. [d] Freezing of 1s electrons.

Table II. Difference in Total Energy,[a] ΔE (hartrees), and Well Depth, MEP Minimum (kcal/mol), of the Molecular Electrostatic Potential and Its Location (au) of H_2O[b]

	ΔE[c]	x	y	z	MEP minimum
		6-31G			
SCF	0.000000	0.00	0.00	2.12	−85.11
CIPSI/G	−0.059207	0.00	0.00	2.13	−84.41
CIPSI/G+S	−0.059954	0.00	0.00	2.13	−84.73
CIPSI/G+M	−0.135936	0.00	0.00	2.15	−80.62
full-CI	−0.136828	0.00	0.00	2.15	−80.50
		6-31G[d]			
SCF	0.000000	0.00	0.00	2.12	−85.11
CIPSI/G	−0.055225	0.00	0.00	2.13	−84.45
CIPSI/G+S	−0.055891	0.00	0.00	2.13	−85.27
CIPSI/G+M	−0.134783	0.00	0.00	2.15	−80.60
full-CI	−0.135905	0.00	0.00	2.15	−80.45

[a] Referred to the energy computed at the SCF level. [b] The molecular geometry is given in ref 32. [c] E_{SCF}(6-31G) = −75.983 992 hartrees. [d] Freezing of 1s electrons.

Electrostatic charges were determined following the scheme reported by Singh and Kollman.[16b,17c] Thus, electrostatic charges were obtained by fitting the point charge electrostatic potentials to the rigorous quantum mechanical (eq 2–4) calculated at points placed on a set of Connolly layers[30] outside the van der Waals radii of the atoms by means of the Levenberg–Marquardt nonlinear optimization procedure.[31]

Results and Discussion

In order to assess the effect of the electron correlation on the molecular electrostatic potential and to determine the goodness of the CIPSI method for computing MEPs, a preliminary study concerning calculations at the SCF, CIPSI, and full-CI levels for HF and H_2O was carried out. Such calculations were performed by using both 6-31G* and 6-31G basis sets. The influence of the

(22) Incorporation of the full-CI program to the HONDO-CIPSI package by J. Rubio and F. Illas, University of Barcelona, February 1989.
(23) Knowles, P. J.; Handy, N. C. *Comput. Phys. Commun.* **1989**, *54*, 75.
(24) (a) Daudey, J. P.; Malrieu, J. P. In *Current Aspects of Quantum Chemistry 1981*; Carbó, R., Ed.; Elsevier: Amsterdam, 1982; p 35. (b) Cimiraglia, R.; Persico, M. *J. Comput. Chem.* **1987**, *8*, 39. (c) Rubio, J.; Ricart, J. M.; Illas, F. *J. Comput. Chem.* **1988**, *9*, 836. (d) Illas, F.; Rubio, J.; Ricart, J. M. *J. Chem. Phys.* **1988**, *89*, 6376.
(25) (a) Epstein, P. S. *Phys. Rev.* **1926**, *28*, 695. (b) Nesbet, R. K. *Proc. R. Soc. London, A* **1955**, *230*, 312. (c) Nesbet, R. K. *Proc. R. Soc. London, A* **1955**, *230*, 322.
(26) (a) Lowdin, P. O. *Phys. Rev.* **1955**, *97*, 1474. (b) Davidson, E. R. *Rev. Mod. Phys.* **1972**, *42*, 451.
(27) Hehre, W. J.; Ditchfield, R.; Pople, J. A. *J. Chem. Phys.* **1982**, *56*, 2257.
(28) Hariharan, P. C.; Pople, J. A. *Theor. Chim. Acta* **1973**, *28*, 213.
(29) (a) Kuipers, G. A.; Smith, D. F.; Nielsen, A. N. *J. Chem. Phys.* **1956**, *25*, 275. (b) Herzberg, G. *Molecular Spectra and Molecular Structure I. Spectra of Diatomic Molecules*; Van Nostrand: New York, 1950. (c) Herzberg, G. *Molecular Spectra and Molecular Structure III. Electronic Spectra and Electronic Structure of Polyatomic Molecules*; Van Nostrand: New York, 1966. (d) Takagi, K.; Oka, T. *J. Phys. Soc. Jpn.* **1963**, *18*, 1174. (e) Lister, D. G.; Tyler, J. K.; Hog, J. H.; Larson, N. W. *J. Mol. Struct.* **1974**, *23*, 253.
(30) Connolly, M. *QCPE Bull.* **1981**, *1*, 75.
(31) Press, W. H.; Flannery, B. P.; Teukolsky, S. A.; Vettering, W. T. *Numerical Recipes*; Cambridge University Press: Cambridge, 1986.
(32) HF: F (0.,0.,0.), H (1.733,0.,0.). N_2: N (0.,0.,−1.034), N (0.,0.,1.034). CO: C (0.,0.,0.), O (0.,0.,2.132). HCN: C (0.,0.,0.), N (2.181,0.,0.), H (−2.009,0.,0.). H_2O: O (0.,0.,0.), H (1.430,0.,−1.107), H (−1.430,0.,−1.107). CH_2O: C (0.,0.,0.), O (0.,0.,2.283), H (1.792,0.,−1.112), H (−1.792,0.,−1.112). Coordinates are given in atomic units.

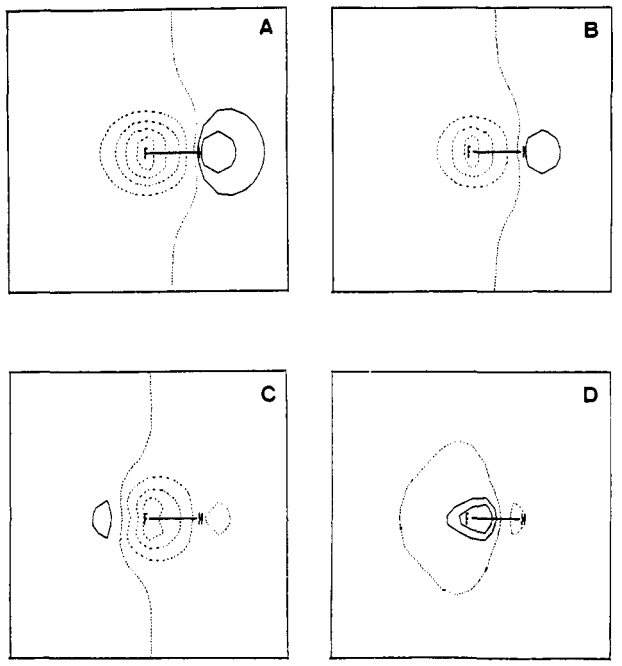

Figure 1. Difference maps of the molecular electrostatic potentials for HF computed from SCF, CIPSI/G, CIPSI/G+S, CIPSI/G+M, and full-CI computations performed by using the 6-31G* basis set. Plots are obtained from the difference between the full-CI MEP and the SCF or CIPSI MEP. Solid lines indicate negative contours, and dashed lines indicate positive contours. The plots and the values (kcal/mol) of the contours are (A) CI vs SCF MEPs (-4.,-2.,0.,5.,10.,15.,20.), (B) CI vs CIPSI/G MEPs (-3.,0.,5.,10.,15.), (C) CI vs CIPSI/G+S MEPs (-1.,0.,2.,5.,8.), and (D) CI vs CIPSI/G+M MEPs (-0.2,-0.1,0.,0.1.).

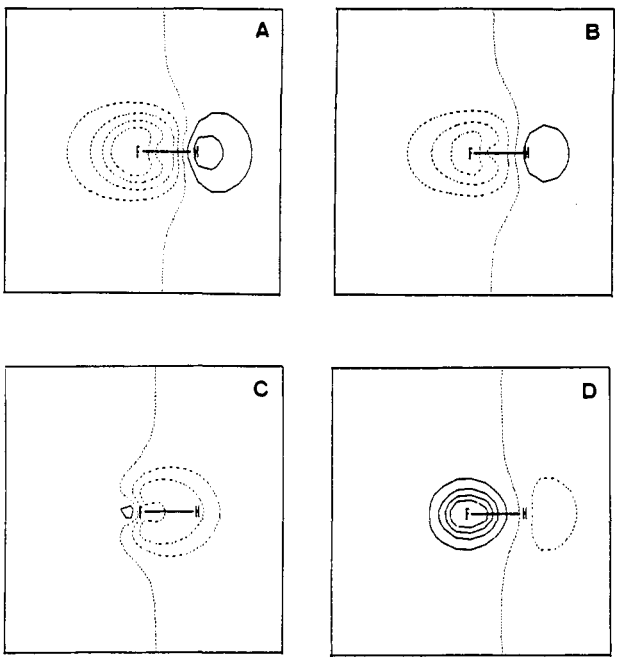

Figure 2. Difference maps of the molecular electrostatic potentials for HF computed from SCF, CIPSI/G, CIPSI/G+S, CIPSI/G+M, and full-CI computations performed by using the 6-31G basis set without the frozen-core approximation. Plots are obtained from the difference between the full-CI MEP and the SCF or CIPSI MEP. Solid lines indicate negative contours, and dashed lines indicate positive contours. The plots and the values (kcal/mol) of the contours are (A) CI vs SCF MEPs (-6.,-3.,0.,3.,6.,9.,12.), (B) CI vs CIPSI/G MEPs (-3.,0.,3.,6.,9.), (C) CI vs CIPSI/G+S MEPs (-2.,0.,2.,4.), and (D) CI vs CIPSI/G+M MEPs (-0.8,-0.6,-0.4,-0.2,0.,0.1.).

frozen-core approximation was also evaluated at both CIPSI and full-CI computational levels in the calculations carried out with the 6-31G basis set.

Tables I and II show the well depth and the location of the MEP minimum for HF and H_2O, respectively. The results in Tables I and II show that very slight differences in the well depth and in its location appear when the MEP minima determined from SCF and full-CI calculations are compared, irrespective of the quality of the basis set. Thus, the absolute value of the MEP minimum for HF decreases 1.61 and 2.91 kcal/mol when the electron correlation is completely taken into account in computations performed at the 6-31G* and 6-31G levels, respectively. However, the distance from the molecule to the MEP minimum undergoes an increase of approximately 0.01 Å in the full-CI calculations with respect to the SCF results. Likewise, the absolute value of the MEP minimum for H_2O evaluated from the full-CI wave function computed by using the 6-31G basis set decreases 4.61 kcal/mol with regard to the SCF MEP minimum, whereas the distance from the oxygen atom to the MEP minimum is increased by approximately 0.02 Å.

Results obtained from CIPSI computations (Tables I and II) gradually tend to the full-CI values as the number of determinants included in the wave function increases, i.e., as the wave function becomes more correlated. Thus, while the CIPSI/G results are very close to the SCF ones, the energy value and location of the MEP minimum derived from the CIPSI/G+M calculations are in practice identical with the full-CI values.

Results in Tables I and II also show that no significant differences are detected when results obtained with and without the frozen-core approximation are compared. Accordingly, the freezing of the inner electrons seems to have no effect on the modulation of the electron correlation on the well depth or the location of the MEP minimum.

Results mentioned above only concern the influence of the electron correlation on the characteristics of the MEP minimum, since usually the main interest of the MEP lies in the well depth and in the location of the MEP minimum. Nevertheless, we also analyzed the effect of the electron correlation on the electrostatic potential distribution in the whole space surrounding the molecule. For this purpose, the MEP maps for HF and H_2O computed from SCF, CIPSI, and full-CI calculations were determined, and the differences between SCF and CIPSI MEPs with regard to the full-CI MEP are represented as MEP difference maps in Figures 1-3.

Simple analysis of Figures 1-3 reveals that the SCF MEP exhibits the largest differences with regard to the full-CI MEP and that such differences decrease as the wave function becomes more correlated. Inspection of the difference maps between full-CI and SCF MEPs (Figures 1a, 2a, and 3a) clearly shows that electron correlation shifts electron density from fluorine and oxygen to hydrogens, this trend also being reflected in the full-CI vs CIPSI/G MEP difference maps (see Figures 1b, 2b, and 3b). Nevertheless, the difference map between full-CI vs CIPSI/G+S MEPs for HF exhibits a different behavior from that determined for H_2O: While the difference map for H_2O implies an electron density transfer from oxygen to hydrogens, the map for HF points out a reverse effect (see Figures 1c, 2c, and 3c). A similar, even much less remarkable situation is also observed in the maps corresponding to differences between the MEPs evaluated from full-CI and CIPSI/G+M computations (see Figures 1d, 2d, and 3d).

For a more exact quantification of the differences between MEPs computed from the SCF, CIPSI, and full-CI wave functions, the respective MEPs for HF and H_2O were evaluated at these computational levels in a set of points (approximately 200) placed on a layer located at a distance from the nuclei ranging from 0.05 to 3 Å. Results are displayed in Figure 4, which shows the variation of the root mean square deviation of the MEPs determined at the SCF and CIPSI levels with regard to the full-CI MEP on the distance from the nuclei to the layer.

Analysis of Figure 4 indicates that the electron correlation has a different influence depending upon the distance from the nuclei. Thus, the profiles for both HF and H_2O exhibit two well-differentiated regions, the border between the inner region and the outer being approximately placed at a distance of 1.1-1.3 Å from

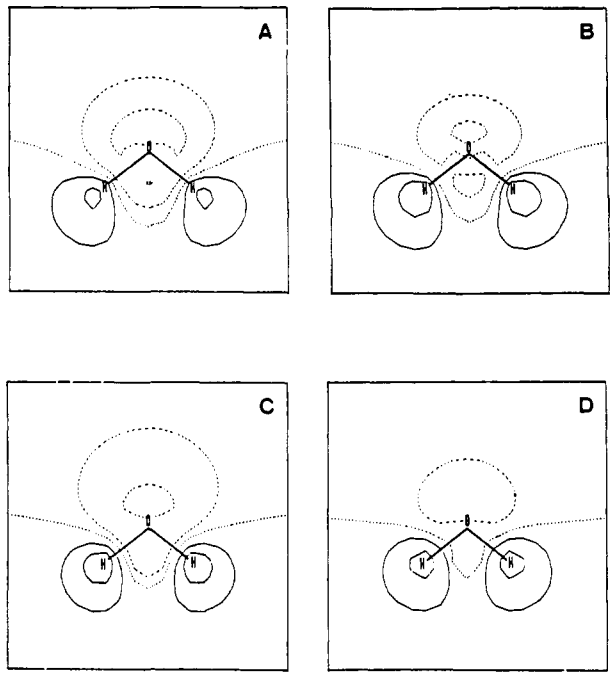

Figure 3. Difference maps of the molecular electrostatic potentials for H_2O computed from SCF, CIPSI/G, CIPSI/G+S, CIPSI/G+M, and full-CI computations performed by using the 6-31G basis set without the frozen-core approximation. Plots are obtained from the difference between the full-CI MEP and the SCF or CIPSI MEP. Solid lines indicate negative contours, and dashed lines indicate positive contours. The plots and the values (kcal/mol) of the contours are (A) CI vs SCF MEPs (-4.,-2.,0.,3.,8.), (B) CI vs CIPSI/G MEPs (-4.,-2.,0.,4.,8.), (C) CI vs CIPSI/G+S MEPs (-6.,-3.,0.,2.,6.), and (D) CI vs CIPSI/G+M MEPs (-0.3,-0.1,0.,0.1).

the nuclei, which could be approximately ascribed to the van der Waals radii of the atoms in the molecule. The root mean square deviation profiles of the outer region correspond to a "plateau", the root mean square deviation being very small. However, the profiles of the inner region tend to increase as the layer is shifted from 1.1 Å to the nuclei. This increase in the rms deviation is less notable and in some cases changes to a decrease when the layer is located close to the nuclei.

These results indicate that the electron correlation mainly modulates those regions of the space closest to the nuclei, its effect being very slight outside the van der Waals sphere of the molecule. The MEP difference maps reported in Figures 1–3 confirms this, which can be easily explained bearing in mind that the molecular electron density is relatively high and changes rapidly with distance near the nuclei,[1a,b] and consequently the effect of the introduction of the electron correlation into the wave function will be greater in the inner region.

The small effect of the electron correlation outside the van der Waals spheres of molecules is of major importance, since it supports the goodness of the SCF MEPs in the outer regions, which are precisely where the MEP dominates the intermolecular interactions. It is worthwhile to note that these regions are the zones where the sites and the pathways of chemical reactivity begin to be defined.

According to results displayed in Table I and Figure 4, another noticeable aspect is that the change of the MEP originated from the introduction of the single excitations into the wave function need not be reflected in a corresponding variation in the energy of the molecule; i.e., although the contribution of single excitations to the energy is expected to be neglibible, their influence on the molecular properties can not be ruled out a priori.

A simple inspection of Figure 4 indicates the reliability of the CIPSI/G+M method to reproduce, almost exactly, the MEP determined from the full-CI wave function in all the space surrounding the molecule, as can also be stated from the values of the contours drawn in the MEP difference maps displayed in Figures 1d, 2d, and 3d. In this respect, note that the determinants included in the wave function obtained from the CIPSI method have been selected according to their contribution to the first-order wave function. Moreover, comparison of Figure 4b–e, which corresponds to computations for HF and H_2O without (4b,d) and with (4c,e) the frozen-core approximation, demonstrated that the freezing of the inner electrons has no effect on the MEP evaluated in the whole space, as was previously noted for the MEP minimum. This result is clearly pointed out in Figure 5, which displays the variation of the root mean square deviation of the full-CI MEPs determined with and without the frozen-core approximation on the distance from the nuclei to the layer. Thus, Figure 5a,b, which corresponds to the molecules of HF and H_2O, respectively, indicates that the root mean square deviation is lower than 0.1 and 0.04 kcal/mol when regions located 0.5 Å from the nuclei are considered, a maximum deviation of only 0.45 and 0.40 kcal/mol being reached near the nuclei. This finding can easily be explained by considering that the determinants originating from the excitations of the 1s electrons of non-hydrogen atoms have a very small contribution to the wave function. In fact, the occupancies of the lowest occupied molecular orbital for HF and H_2O according to the full-CI calculation performed by using the 6-31G basis set without the frozen-core approximation are 1.999969 and 1.999959 electrons, respectively. Therefore, the frozen-core approximation does not introduce any significant change with respect to either the MEP minimum or the essential features of the MEP maps. Nevertheless, it must be pointed out that the inclusion of core electrons can be important to study other properties.[33]

Another interesting aspect to be discussed concerns the extent of the dependence of the MEP on the electron correlation with regard to the variation on the quality of the basis set. When the SCF results are compared to the full-CI ones, note that the absolute value of the MEP minimum for HF decreases 1.61 and 2.91 kcal/mol in the 6-31G* and 6-31G calculations, whereas the well depth increases (in absolute value) approximately 10 kcal/mol when polarization functions are added to the 6-31G basis set, whatever the computational level considered (see Table I). Similarly, the absolute value of the full-CI MEP minimum for H_2O is 4.61 kcal/mol less than the SCF one when the 6-31G basis set is used (see Table II), whereas the MEP minimum evaluated from calculations at the 6-31G level is approximately 22 kcal/mol deeper than the MEP minimum derived from computations carried out by using the 6-31G* basis set, irrespective of the level of calculation (see Tables II and III). Likewise, the location of the MEP minimum is also more influenced by the quality of the basis set than by the introduction of electron correlation. For instance, the introduction of the electron correlation causes a separation of the MEP minimum from the molecule of approximately 0.01 Å for HF and 0.02 Å for H_2O, whereas the inclusion of polarization functions to the 6-31G basis set leads to a separation of the MEP minimum of around 0.05 and 0.09 Å, respectively. This finding suggests that, in general, the quality of the basis set employed in the computation of the SCF wave function has an effect on the MEP minimum characteristics that is much more pronounced than the influence of the electron correlation.

As a summary of the preceding discussion, it can be concluded that inner electrons have a negligible contribution to the effect of electron correlation of the modulation of the MEP and that the wave function obtained at the CIPSI/G+M level accurately reproduces the characteristics of the MEP minimum as well as the essential fine features of the MEP maps determined from the full-CI wave function, but at a largely reduced computational cost. Indeed, the influence of the quality of the basis set in modulating the MEP is more relevant than the effect of the electron correlation.

Bearing in mind the conclusions noted above, we computed the MEPs for HF, N_2, CO, HCN, H_2O, and CH_2O obtained from SCF, CIPSI/G, and CIPSI/G+M calculations carried out by using the 6-31G* basis set and the frozen-core approximation to assess in a more extended set of molecules the dependence of the

(33) Bauschlicher, C. W., Jr.; Langhoff, S. R.; Taylor, P. R. *J. Chem. Phys.* **1988**, *88*, 2540.

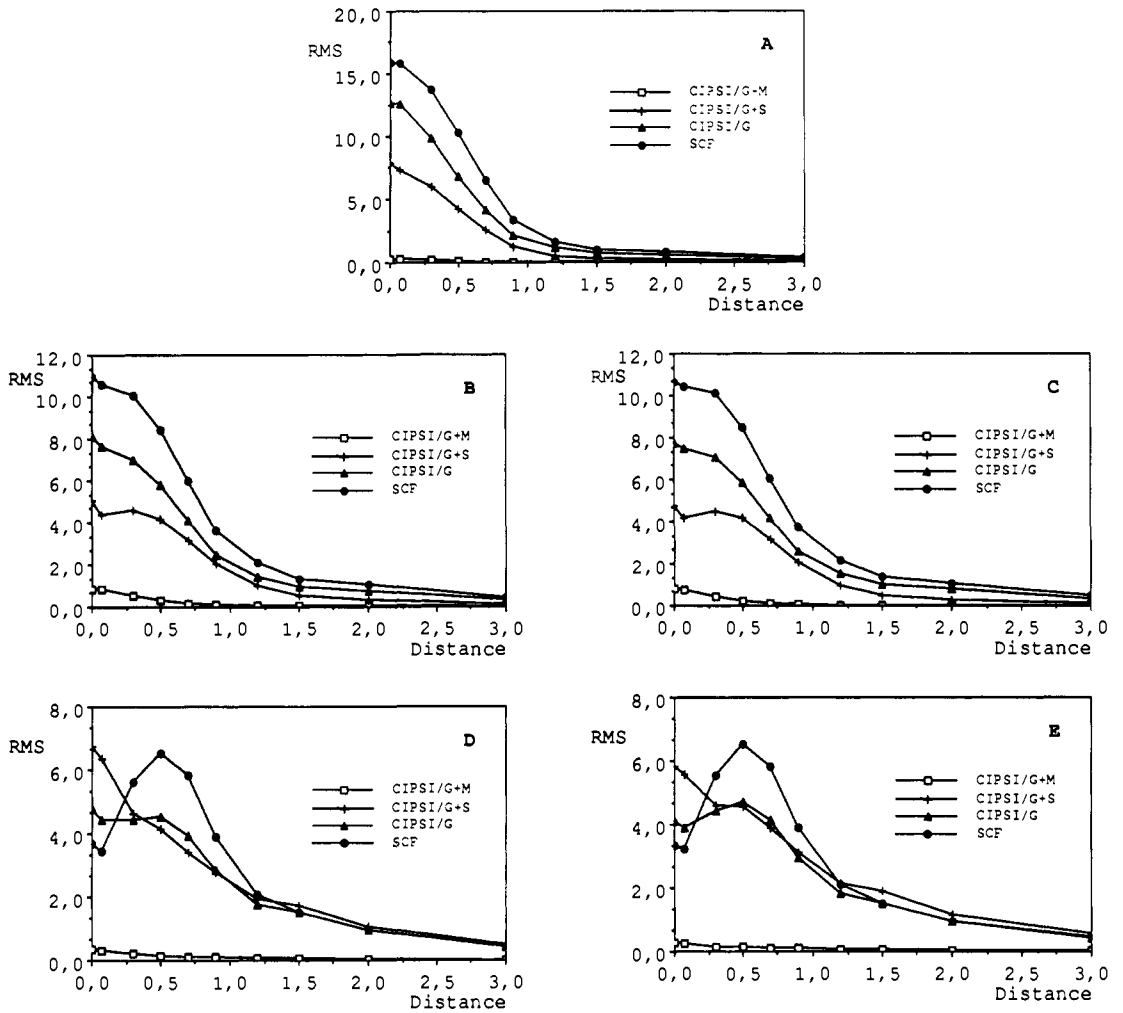

Figure 4. Profiles of the variation on the distance (Å) from the nuclei of the root mean square deviation (kcal/mol) of the MEP determined from SCF, CIPSI/G, CIPSI/G+S, and CIPSI/G+M calculations with regard to the full-CI MEP: (A) MEP for HF at the 6-31G* level with the frozen-core approximation, (B) MEP for HF at the 6-31G level without the frozen-core approximation, (C) MEP for HF at the 6-31G level with the frozen-core approximation, (D) MEP for H_2O at the 6-31G level without the frozen-core approximation, and (E) MEP for H_2O at the 6-31G level with the frozen-core approximation.

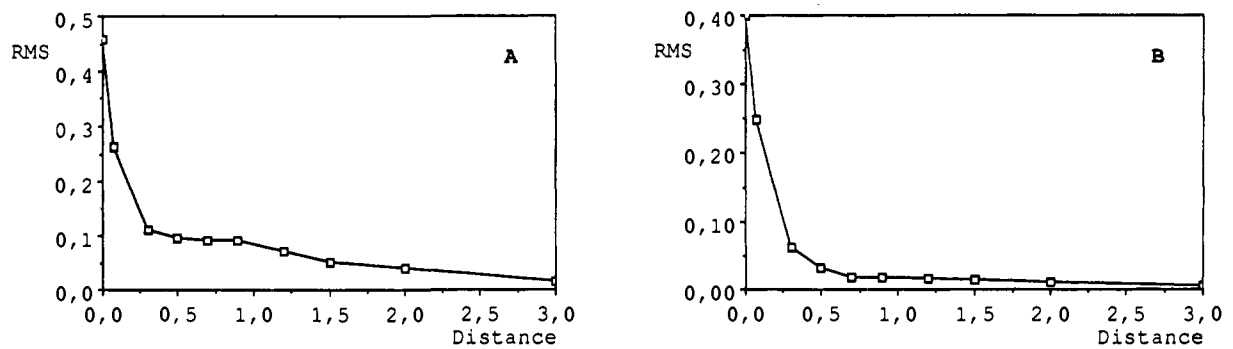

Figure 5. Profiles of the variation on the distance (Å) from the nuclei of the root mean square deviation (kcal/mol) of the MEP determined from full-CI calculations with and without the frozen-core approximation: (A) MEP for HF at the 6-31G level and (B) MEP for H_2O at the 6-31G level.

MEP on the electron correlation.

Table III reports the well depth and the location of the MEP minima for HF, N_2, CO, HCN, H_2O, and CH_2O computed at the SCF, CIPSI/G, and CIPSI/G+M levels. The SCF wave function provides in general a reliable description of the MEP minimum, since both the well depth and the location suffer a very small change when the electron correlation is introduced into the wave function. Thus, the variation of the MEP minimum for HF, H_2O, N_2, and HCN is lower than 2 kcal/mol when the SCF results are compared with the CIPSI/G+M values, whereas a change of near 6 kcal/mol is found for CH_2O and CO. On the other hand, the largest variation in the location of the MEP minimum due to the electron correlation is lower than 0.06 Å.

The influence of the electron correlation on the MEP is especially noticeable for CO. For this molecule, the inclusion of electron correlation modifies not only the depth of the MEP minima located near the carbon and the oxygen atoms, but also their relative magnitude. Thus, the MEP minimum close to the carbon atom is only 3 kcal/mol deeper than that of the oxygen atom at the SCF level, but the introduction of the electron correlation either at the CIPSI/G or CIPSI/G+M levels notably shifts electron density from oxygen to carbon, the MEP well depth of this latter atom being about 3 times higher than that of oxygen. Therefore, the electron correlation must be taken into account

Table III. Difference in Total Energy,[a] ΔE (hartrees), and Well Depth, MEP Minimum (kcal/mol), of the Molecular Electrostatic Potential and Its Location (au)[b]

	ΔE[c]		x	y	z	MEP minimum
		HF				
SCF	0.000000		−1.15	0.00	−1.97	−34.48
CIPSI/G	−0.089950		−1.14	0.00	−1.99	−33.88
CIPSI/G+M	−0.183613		−1.10	0.00	−2.02	−32.87
		N_2				
SCF	0.000000		0.00	0.00	−3.90	−11.23
CIPSI/G	−0.180243		0.00	0.00	−3.87	−12.47
CIPSI/G+M	−0.311142		0.00	0.00	−3.87	−12.97
		CO				
SCF	0.000000	(C)	0.00	0.00	−2.80	−17.56
		(O)	0.00	0.00	4.87	−14.48
CIPSI/G	−0.152583	(C)	0.00	0.00	−2.77	−22.28
		(O)	0.00	0.00	5.04	−7.53
CIPSI/G+M	−0.286730	(C)	0.00	0.00	−2.80	−20.51
		(O)	0.00	0.00	4.98	−8.88
		HCN				
SCF	0.000000		4.69	0.00	0.00	−48.09
CIPSI/G	−0.152479		4.68	0.00	0.00	−48.83
CIPSI/G+M	−0.289207		4.70	0.00	0.00	−46.75
		H_2O[d]				
SCF	0.000000		0.00	0.00	2.30	−60.93
			0.00	−1.49	1.69	−62.81
CIPSI/G	−0.085456		0.00	0.00	2.31	−60.63
			0.00	−1.48	1.71	−62.41
CIPSI/G+M	−0.193610		0.00	0.00	2.31	−59.14
			0.00	−1.53	1.67	−61.26
		CH_2O[d]				
SCF	0.000000		1.84	0.00	3.71	−49.23
			0.00	0.00	4.75	−43.11
CIPSI/G	−0.172260		1.87	0.00	3.74	−42.38
			0.00	0.00	4.80	−36.74
CIPSI/G+M	−0.310193		1.88	0.00	3.73	−42.76
			0.00	0.00	4.80	−37.17

[a] Referred to the energy computed at the SCF level. [b] The SCF calculations were carried out with the 6-31G* basis set. 1s electrons were kept frozen in CIPSI computations. The molecular geometries are given in ref 32. [c] E_{SCF}(6-31G*) = −100.000747 (HF); −108.942313 (N_2); −112.736786 (CO); −92.873275 (HCN); −76.009138 (H_2O); and −113.863737 (CH_2O) hartrees. [d] The MEP minima in both the plane of the molecule and the perpendicular plane are reported.

to obtain a correct picture of the electrostatic potential distribution for CO.

When results displayed in Table III are analyzed in detail, it is clear that the effect of the electron correlation on the MEP minimum is not necessarily the decrease of the well depth. Moreover, the variation of the MEP minimum well depth is only a consequence of the change of the electron distribution occurring when a many-determinantal wave function is considered. Thus, the variation of the absolute value of the MEP minima reported in Table III can be easily understood from the analysis of the difference maps between the MEPs determined from the wave functions computed at the SCF and CIPSI/G+M levels displayed in Figure 6. The MEP difference maps for HF and H_2O indicate that electron correlation shifts electron density from fluorine and oxygen to hydrogens, and for CH_2O the electron density is transferred from oxygen to carbon. Consequently, the corresponding MEP minimum well depths decrease (in absolute values). The decrease of the absolute value of the well depth for HCN is originated from the transfer of electron density from the basin of the nitrogen atom to the bond between carbon and hydrogen and to the region of space close to nitrogen. Similarly, the shift of electron density from the bond to nitrogens in the case of N_2 explains the increase of the absolute value of the MEP minimum. Finally, the transfer of electron density from oxygen to carbon in the case of CO accounts for the enlargement of the difference between the two MEP minima discussed above.

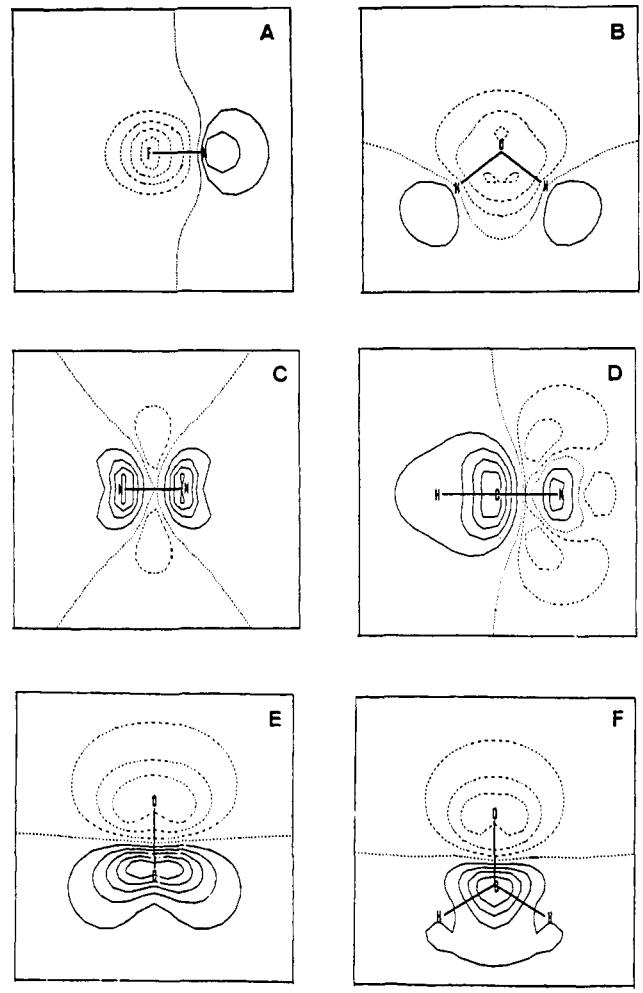

Figure 6. Difference maps of the molecular electrostatic potentials for HF, H_2O, N_2, HCN, CO, and CH_2O computed from SCF and CIPSI/G+M computations performed by using the 6-31G* basis set with the frozen-core approximation. Plots are obtained from the difference between the CIPSI/G+M MEP and the SCF MEP. Solid lines indicate negative contours, and dashed lines indicate positive contours. The plots and the values (kcal/mol) of the contours are (A) HF (−4.,−2.,−.,5.,10.,15.,20.), (B) H_2O (−1.,0.,2.,5.,9.), (C) N_2 (−18.,−14.,−10.,−5.,−.,2.), (D) HCN (−20.,−15.,−10.,−5.,0.,2.,4.), (E) CO (−25.,−20.,−15.,−10.,−5.,0.,5.,10.,15.), and (F) CH_2O (−20.,−15.,−10.,−5.,0.,5.,10.,15.).

Present results point out the reliability of the SCF wave function to determine with a reasonable accuracy both the well depth and the position of the MEP minimum, even though the neglect of the electron correlation effect can no longer remain valid for certain molecules such as CO. Indeed, the MEP determined at the SCF level properly reflects the features of the MEP maps in the space surrounding the molecule except in those regions close to the nuclei, where the influence of the electron correlation must be taken into account.

The study of the effect of the electron correlation on the electrostatic potential distribution of molecules was extended to the atomic charges, since the concept of the atomic charge provides a tool for explaining the molecular reactivity from an intuitive chemical viewpoint. In the present work, both Mulliken and electrostatic charges were considered.

Table IV reports the Mulliken and electrostatic charges of HF computed from SCF, CIPSI, and full-CI calculations performed by using the 6-31G* and 6-31G basis sets. Electron correlation leads to a very slight variation of both Mulliken and electrostatic charges. In fact, the charges determined from the wave function obtained at the CIPSI/G+M levels are nearly identical with those of the full-CI. Thus, the full-CI Mulliken charge of the fluorine atom is decreased in absolute value by 0.0292 and 0.0314 units with regard to the SCF values computed at the 6-31G* and 6-31G

Table IV. Mulliken and Electrostatic Charges (Q_M, Q_E), Dipoles (μ_M, μ_E), and the Exact Dipole Moment (μ) Computed from the Wave Function for HF[a]

	Q_M[b]	Q_E[b]	rms	μ_M	μ_E	μ[c]
		6-31G*				
SCF	−0.5436	−0.4542	0.110	2.394	2.001	1.984
CIPSI/G	−0.5387	−0.4496	0.111	2.373	1.980	1.963
CIPSI/G+S	−0.5261	−0.4326	0.120	2.317	1.906	1.887
CIPSI/G+M	−0.5144	−0.4372	0.115	2.266	1.925	1.907
full-CI	−0.5144	−0.4372	0.115	2.266	1.925	1.907
		6-31G				
SCF	−0.4819	−0.5236	0.037	2.123	2.306	2.296
CIPSI/G	−0.4754	−0.5172	0.038	2.094	2.278	2.267
CIPSI/G+S	−0.4574	−0.4929	0.045	2.015	2.171	2.159
CIPSI/G+M	−0.4497	−0.4994	0.043	1.981	2.200	2.187
full-CI	−0.4505	−0.5001	0.043	1.984	2.203	2.190
		6-31G[d]				
SCF	−0.4819	−0.5236	0.037	2.123	2.306	2.296
CIPSI/G	−0.4754	−0.5172	0.038	2.094	2.278	2.267
CIPSI/G+S	−0.4573	−0.4928	0.045	2.014	2.170	2.158
CIPSI/G+M	−0.4498	−0.4994	0.043	1.981	2.200	2.187
full-CI	−0.4498	−0.4993	0.043	1.981	2.199	2.186

[a] rms is the root mean square deviation of the fitting of the Coulombic potential generated by the electrostatic charges to the quantum mechanical molecular electrostatic potential. Dipole moments are expressed in debyes. [b] Atomic charges of fluorine. [c] Experimental gas-phase dipole moment is 1.82 D. [d] Freezing of 1s electrons.

Table V. Mulliken and Electrostatic Charges (Q_M, Q_E), Dipoles (μ_M, μ_E), and the Exact Dipole Moment (μ) Computed from the Wave Function for H_2O[a]

		Q_M	Q_E	rms	μ_M	μ_E	μ[b]
			6-31G				
SCF	(O)	−0.7917	−0.9454	0.055	2.228	2.660	2.630
	(H)	0.3959	0.4727				
CIPSI/G	(O)	−0.7908	−0.9452	0.056	2.225	2.660	2.629
	(H)	0.3954	0.4726				
CIPSI/G+S	(O)	−0.7837	−0.9500	0.056	2.205	2.673	2.642
	(H)	0.3918	0.4750				
CIPSI/G+M	(O)	−0.7311	−0.9081	0.063	2.058	2.556	2.521
	(H)	0.3656	0.4541				
full-CI	(O)	−0.7296	−0.9069	0.063	2.053	2.552	2.518
	(H)	0.3648	0.4534				
			6-31G[c]				
SCF	(O)	−0.7917	−0.9454	0.055	2.228	2.660	2.630
	(H)	0.3959	0.4727				
CIPSI/G	(O)	−0.7911	−0.9450	0.056	2.227	2.659	2.629
	(H)	0.3956	0.4725				
CIPSI/G+S	(O)	−0.7868	−0.9553	0.056	2.214	2.688	2.657
	(H)	0.3934	0.4776				
CIPSI/G+M	(O)	−0.7311	−0.9080	0.063	2.058	2.555	2.521
	(H)	0.3656	0.4540				
full-CI	(O)	−0.7295	−0.9064	0.063	2.053	2.551	2.517
	(H)	0.3647	0.4532				

[a] rms is the root mean square deviation of the fitting of the Coulombic potential generated by the electrostatic charges to the quantum mechanical molecular electrostatic potential. Dipole moments are expressed in debyes. [b] Experimental gas-phase dipole moment is 1.85 D. [c] Freezing of 1s electrons.

levels, respectively, whereas a decrease of 0.0170 and 0.0235 units is observed when dealing with the electrostatic charge. Results similar to those obtained for HF are also observed when the Mulliken and electrostatic charges of H_2O computed by using the 6-31G basis set are considered (Table V). For instance, the SCF Mulliken charge of the oxygen atom suffers a decrease of 0.0621 units with respect to the full-CI one, whereas such a decrease is of 0.0385 units when the electrostatic charge is considered.

Results shown in Tables IV and V indicate that the freezing of the inner electrons of the fluorine and oxygen atoms does not lead to a significant difference with regard to the Mulliken and electrostatic charges derived from computations performed without the frozen-core approximation. Indeed, note that the quality of the basis set modulates both Mulliken and electrostatic charges more than electron correlation. Thus, either the Mulliken or the electrostatic charges of the fluorine atom vary by approximately 0.064 units when values based on the 6-31G* and 6-31G basis sets are compared (see Table IV), this variation being even greater in the case of the oxygen atom of H_2O, since such a difference reaches a value of nearly 0.12 units (see Tables V and VI). Accordingly, all these findings reflect the trends mentioned above about the influence of the electron correlation on the features of the MEP minimum.

Table VI. Mulliken and Electrostatic Charges (Q_M, Q_E), Dipoles (μ_M, μ_E), and the Exact Dipole Moment (μ) Computed from the Wave Function for HF, CO, HCN, H_2O, and CH_2O[a]

		Q_M	Q_E	rms	μ_M	μ_E	μ[b]
			HF				
SCF	(F)	−0.5436	−0.4542	0.110	2.394	2.001	1.984
	(H)	0.5436	0.4542				
CIPSI/G	(F)	−0.5387	−0.4496	0.111	2.373	1.980	1.963
	(H)	0.5387	0.4496				
CIPSI/G+M	(F)	−0.5144	−0.4372	0.115	2.266	1.925	1.907
	(H)	0.5144	0.4372				
			CO[c]				
SCF	(C)	0.2934	0.0687	0.882	1.590	0.372	0.331
	(O)	−0.2934	−0.0687				
CIPSI/G	(C)	0.2080	−0.0097	0.997	1.127	−0.053	−0.091
	(O)	−0.2080	0.0097				
CIPSI/G+M	(C)	0.1740	−0.0065	0.999	0.943	−0.035	−0.069
	(O)	−0.1740	0.0065				
			HCN				
SCF	(C)	0.0284	0.1132	0.045	3.516	3.195	3.228
	(N)	−0.3438	−0.3543				
	(H)	0.3154	0.2411				
CIPSI/G	(C)	0.0239	0.1512	0.061	3.438	3.062	3.107
	(N)	−0.3343	−0.3601				
	(H)	0.3104	0.2089				
CIPSI/G+M	(C)	−0.0016	0.1871	0.066	3.438	3.062	2.978
	(N)	−0.2798	−0.3620				
	(H)	0.2814	0.1749				
			H_2O				
SCF	(O)	−0.8974	−0.8042	0.110	2.525	2.263	2.219
	(H)	0.4487	0.4021				
CIPSI/G	(O)	−0.8960	−0.8050	0.109	2.522	2.265	2.220
	(H)	0.4480	0.4025				
CIPSI/G+M	(O)	−0.8529	−0.7862	0.113	2.401	2.213	2.165
	(H)	0.4265	0.3931				
			CH_2O				
SCF	(C)	0.1456	0.4156	0.063	3.421	2.755	2.759
	(O)	−0.4442	−0.4554				
	(H)	0.1493	0.0199				
CIPSI/G	(C)	0.0975	0.4079	0.085	2.914	2.276	2.283
	(O)	−0.3697	−0.3973				
	(H)	0.1361	−0.0053				
CIPSI/G+M	(C)	0.0789	0.3924	0.082	2.837	2.331	2.338
	(O)	−0.3546	−0.3987				
	(H)	0.1379	0.0031				

[a] rms is the root mean square deviation of the fitting of the Coulombic potential generated by the electrostatic charges to the quantum mechanical molecular electrostatic potential. Dipole moments are expressed in debyes. The SCF calculations were carried out with the 6-31G* basis set. 1s electrons were kept frozen in CIPSI computations. [b] Experimental gas-phase dipole moments are 1.82 (HF); −0.04 (CO); 2.98 (HCN); 1.85 (H_2O); and 2.33 (CH_2O) D. [c] A positive dipole moment means C^+O^-.

Table VI reports the Mulliken and electrostatic charges for HF, CO, HCN, H_2O, and CH_2O derived from SCF and CIPSI computations performed by using the 6-31G* basis set. In agreement with the preceding discussion, inspection of results in Table VI reveals a very small change of atomic charges as the electron correlation is taken into account in the wave function. The fact that the electron correlation leads to a decrease of atomic charges with regard to the SCF ones can be easily understood bearing in mind the tendency of the electron correlation to counteract the overestimation of the ionic structures by the molecular orbitals methods. In this respect, the dipole moments computed from either Mulliken or electrostatic atomic charges as well as the exact dipole moments calculated from the wave function decrease as the wave function becomes more correlated (see Tables VI–VI), their

corresponding values approaching the experimental gas-phase ones, whatever the quality of the basis set used in the computation of the wave function. It can also be stated from results for HF and H_2O in Tables IV-VI the well-known tendency of the *split-valence* basis sets to overestimate the magnitude of the dipole moment.[34]

Even though the variation of the dipole moment due to the electron correlation is small, let us emphasize the relevance of the introduction of the electron correlation into the wave function in order to obtain reliable dipole moments at least for some molecules, such as the molecule of CO (see Table VI). Note that, for this molecule, the electron correlation not only reduces the dipole moment considerably, but also changes its sign, which when electron correlation is considered accurately reproduces both the magnitude and the orientation of the experimental gas-phase value.

Finally, results suggest that the dipole moment calculated from the electrostatic charges correctly reflects the magnitude and the orientation of the dipole moment rigorously computed from the wave function, irrespective of the computational level considered. This finding, which points out the higher quality of the electrostatic charges with regard to the Mulliken ones, is especially remarkable in the case of CO. Note that the electron correlation changes the sign of the electrostatic charges of the carbon and oxygen atoms at both CIPSI/G and CIPSI/G+M levels, the corresponding electrostatic dipole moments being very close to the quantum mechanical ones as well as to the experimental value. On the contrary, this change is not observed when dealing with the Mulliken charges.

Conclusion

The preceding discussion points out the reliability of the CIPSI method to quantitatively reproduce the effects of the electron correlation on the electrostatic potential distribution in molecules. Thus, the well depth and location of the MEP minima and the fine essential features of the MEP maps for HF and H_2O, as well as atomic charges and dipoles, determined from CIPSI computations performed by considering the $\{G\} + \{M\}$ space agrees near exactly with those evaluated from full-CI calculations, but at a greatly reduced computational cost. Moreover, the freezing of the inner electrons of non-hydrogen atoms has no significant influence on the modulation of the MEP by the electron correlation.

When MEPs determined at the SCF level are considered, electron correlation generally leads to a small change of the MEP minimum, even though this variation can be nonnegligible for certain molecules, such as CO. In this respect, results demonstrate that the quality of the basis set is of greater importance than the inclusion of the electron correlation. The analysis of MEP maps and profiles indicate that the electron correlation does not have a uniform effect on the electrostatic potential in the whole space surrounding the molecule. Thus, electron correlation has a sizeable influence in those regions near the nuclei, but the MEP computed in regions outside the molecular van der Waals sphere remains largely unaffected by electron correlation. Consequently, the wave function determined at the SCF level is able to reflect with a reasonable accuracy the features of the MEP in the outer regions. It is worth noting that electrostatics dominate the intermolecular interactions in this region.

Acknowledgment. We are indebted to Dr. J. Tomasi and R. Cimiraglia for making available the MEP computer program developed by the Pisa group, which was modified to carry out the present work. We thank the Centre de Càlcul de la Universitat de Barcelona for computational facilities.

Registry No. HF, 7664-39-3; N_2, 7727-37-9; CO, 630-08-0; HCN, 74-90-8; H_2O, 7732-18-5; CH_2O, 50-00-0.

(34) (a) Ditchfield, R.; Hehre, W. J.; Pople, J. A. *J. Chem. Phys.* **1971**, *54*, 724. (b) Binkley, J. S.; Pople, J. A.; Hehre, W. J. *J. Am. Chem. Soc.* **1980**, *102*, 939. (c) Gordon, M. S.; Binkley, J. S.; Pople, J. A.; Pietro, W. J.; Hehre, W. J. *J. Am. Chem. Soc.* **1982**, *104*, 2797.

A Theoretical Study of Polyelectrolyte Effects in Protein-DNA Interactions: Monte Carlo Free Energy Simulations on the Ion Atmosphere Contribution to the Thermodynamics of λ Repressor-Operator Complex Formation

B. Jayaram, F. M. DiCapua, and D. L. Beveridge*

Contribution from the Department of Chemistry, Hall-Atwater Laboratories, Wesleyan University, Middletown, Connecticut 06457. *Received October 1, 1990*

Abstract: We report herein a theoretical calculation of the ion atmosphere contribution to the free energy of association for a protein-DNA complex based on Monte Carlo computer simulations and thermodynamic perturbation theory. The system considered is the dimer of the amino-terminal fragment of the λcI repressor in a complex with a 17 base pair oligonucleotide of DNA, based on the crystal structure of Pabo and Sauer. Only the movements of the small ions (sodium and chloride ions) are considered explicitly, with solvent water modeled as a dielectric continuum (a "primitive model"). The free energies are determined as a function of both distance of separation between the protein and the DNA, each of which is fixed in its respective crystal geometry, and ionic strength at a temperature of 298 K. Results of our simulations indicate that the ion atmosphere contribution to the free energy of association is favorable only at short distances of separation and is at a maximum when the protein approaches the DNA from a distance of ~7 Å. This distance corresponds to the radius of the shroud of condensed counterions around B-DNA. At larger distances of separation between the protein and the DNA, the uncondensed diffuse ionic cloud opposes complexation. The effect known as "counterion release" in the context of DNA-ligand association appears to be short-ranged and a property of the condensed counterions only.

Introduction

The nature of protein-DNA interactions is currently a subject of considerable research interest in molecular biophysics.[1-5] Crystal structures of the protein-nucleic acid complexes reported in the recent literature[6-12] and the concurrent 2D NMR studies[13,14]

(1) Pabo, C. O.; Sauer, R. T. *Annu. Rev. Biochem.* **1984**, *53*, 293-321.
(2) Matthews, B. W. *Nature* **1988**, *335*, 294-295.
(3) Travers, A. A. *Annu. Rev. Biochem.* **1989**, *58*, 427-452.

0002-7863/91/1513-5211$02.50/0